

WAVE SETUP VARIATIONS ALONG A CROSS-SHORE PROFILE OF A MACROTIDAL SANDY EMBAYED BEACH, PORSMILIN, BRITTANY, FRANCE

C. Caulet¹, F. Floc'h¹, N. Le Dantec², M. Jaud¹, E. Augereau¹, F. Ardhuin³, C. Delacourt¹

Abstract

We investigated the evolution of the wave setup on a natural sandy pocket beach located on the French Atlantic coast. The wave setup is the increase of the still water level due to the transfer of momentum induced by wave breaking. Numerous studies have examined the role of environmental parameters on the wave setup, on both theoretical and field laboratory environments. They have led to several empirical formulas, frequently used in coastal engineering. Although these formulas are designed to fit with a large variability of natural sites, they show contrasted results. In this paper we aim to determine the abilities to such formulae to bring useable information on water level measurement on our studied site. According to an in situ dataset, we analyze the evolution of these levels under the influence of the beach morphology such as the slope, as well as the tidal modulation, significant in this coastal area.

Key words: Remote sensing, Wave setup, Wave runup, Tidal modulation, swash dynamic

1. Introduction

For decades, the setup has been shown to be of high importance to design littoral features, to assess flooding hazard event or in order to address morphodynamics comprehension (Bowen et al, 1968; Stockdon et al, 2006). In the latter case, the setup occurring all over the intertidal zone interests researchers addressing understanding of the whole intertidal profile dynamics. Since the eighties, the camera system has been broadly used as a continuous and autonomous remote sensing device. It provides a simple way to monitor the nearshore processes, such as water level and wave dynamics (Holman et al., 1993). Numerous studies have been conducted to assess the ability of such device to provide bathymetric and morphologic measurements (Dailloux et al., 2010 ; Holman et al. 2013). Nevertheless these processings need to be improved in certain environments, such as macrotidal site (Bergsma et al. 2016).

Our research goal is to use the wave setup calibrated formula for topographic surveys of the beach directly from the waterline detection via the video system, knowing the still water level (SWL). Hence to have a good assessment of the wave setup all along a cross-shore transect is required in order to minimize the uncertainties on the resulting intertidal topography. However, few studies deal with the quantification of the setup according to tide phase and different conditions on the same beach (e.g. local slope, water table level, grain size). The parameters such as the slope are usually taken as an averaged value for the whole beach. This is potentially problematic knowing that the morphology in energetic environment (e.g. macrotidal, strong wave condition) could face huge changes (i.e. few tens centimeters) during one tide (Floc'h et al. 2016). It possibly introduces huge uncertainties on the water levels assessments and thus on the beach morphology.

The water levels vary with the beach morphology and the hydrodynamics processes occurring in the nearshore. Battjes (1974) shows that the setup and the runup seem to be driven by a single similarity parameter (Battjes, 1974) called the Iribarren number (noted ξ_0) and defined in the following equation (Eq. 1, where β is the beach slope, H_0 is the offshore wave height and λ_0 is the offshore wavelength).

¹ Domaines Océaniques UMR6538, IUEM/UBO, 29280 Plouzané, France, charles.caulet@univ-brest.fr

² CEREMA—Centre d'Etudes et d'expertise sur les Risques, l'Environnement, la Mobilité et l'Aménagement, DTecEMF, F-29280 Plouzané, France

³ LOPS UMR6523, IUEM/IFREMER/UBO fabrice.ardhuin@univ-brest.fr

$$\xi_0 = \frac{\tan(\beta)}{\sqrt{H_0/\lambda_0}} \quad (1)$$

The Iribarren number is a non-dimensional number giving information about the beach morphologic properties and the wave forcing. It compares the beach and the wave steepness and therefore gives a commonly accepted parameter to characterize the reflective ($\xi_0 > 0,3$) and dissipative ($\xi_0 < 0,3$) behavior of the beach.

Numerous field experiments have been designed to measure the wave setup variation on natural beaches. These surveys have been conducted on several environments: gently sloping (Guza and Thornton, 1981); gently sloping and macro-tidal (King et al., 1990); reflective beach (Holman and Sallenger, 1985); mild slope and meso-tidal site under extreme conditions (Senechal et al., 2011); varying slope (dissipative / reflective beach) and macro-tidal (Suanez et al., 2015). Moreover Stockdon et al. (2006) has conducted a study on a wide variability of natural site, gathering data from previous field experiments (Stockdon et al. 2006). From these studies empirical formulations have been drawn to represents the links between the wave setup (noted $\bar{\eta}$) and runup exceedance (noted $R_{X\%}$, where X% represents here the percentage of the runup level exceedance) with environmental parameters, such as the offshore significant waves. The field experiments have been conducted on several sites representing a large variability of environments, nevertheless the results were contrasted.

We propose in this study to examine the variation of the setup, the runup exceedance and the significant swash height (defined below) regarding to the slope, the water level and the wave energy spectra. The first part of the paper describes the dataset used in this study. We detail the processing done to extract the setup and the runup on our site using a camera system. A validation of these measured levels is also discussed. The second part introduces the results we get. The results are discussed in the third part of the study.

2. Dataset and Methods

2.1. Study site

The study site is a small macro-tidal sandy beach called Posmilin, nested in the bay of Bertheaume in the French Atlantic coast (Brittany, France, figure 1).

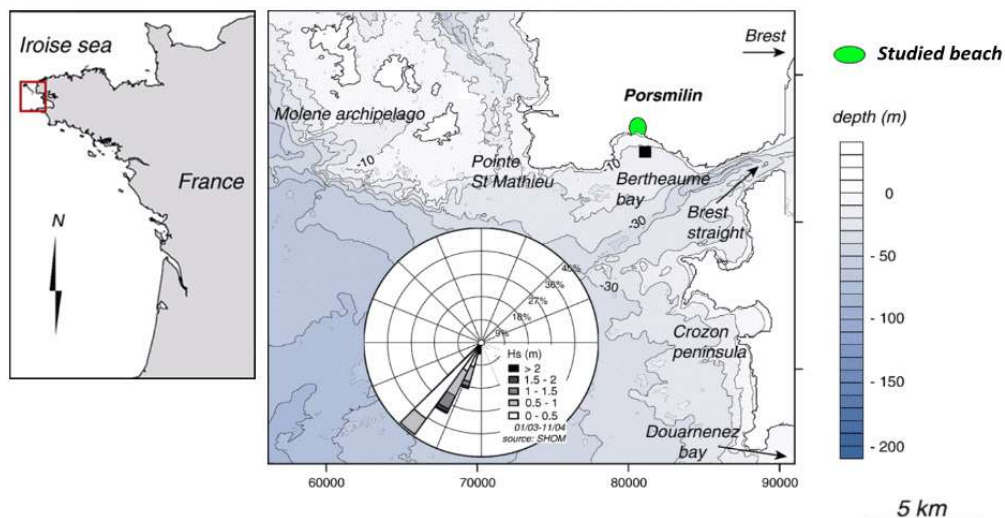


Figure 1. The Posmilin beach is located on the French Atlantic coast, sheltered in the Bertheaume's bay (highlighted by the green spot in the left panel). The swells are mainly south-west (SHOM database) and presents mild energetic conditions (annual significant wave height average equals to 0.5 m), Dehouck, 2006.

The Porsmilin beach is closely monitored by our laboratory since 15 years, in the framework of the National Service of Observation DYNALIT and European service ILLICO. The beach is bounded in both sides by rocky headlands and bounded at the top by a sandy berm. The beach faces the Iroise Sea. The environment is highly energetic, but because of the shallow depth of the shelf (few tens meters) and numerous headlands, shoals and islands, a large amount of this energy is lost in refraction and diffraction process when the swell propagates to the coast. The mean speed of spring tidal currents is 0.4 m/s off the beaches, in Bertheaume's cove (SHOM, 1994). The swell has then a quasi-normal incidence on the beach. The wave conditions are mild with an annual mean significant wave height equals to 0.5 meters. During a storm event the typically significant wave heights reach 1.5 m. The beach could face extremely high energetic conditions during winter storm ($H_s > 5$ m and $T_p > 15$ s) which impact considerably the beach morphology.

The site is under a semi-diurnal and symmetrical macro-tidal regime with a tide range reaching almost seven meters during a spring tide. The beach is alternatively under a tidal dominance ($RTR > 15$) and a low tide terrace type, according to the Masselink & Short (1993) classification (Masselink and Short, 1993) (dimensionless fall velocity always < 2). The beach morphology is characterized by a slope discontinuity located around the MHWN. The mean beach slope at the upper beach is 0.07 and 0.03 at the lower beach (from the averaged DGPS profiles over 13 years). The median sand size is around 300 μm at the intertidal zone (Dehouck, 2006 ; Jaud, 2011 ; Floc'h et al. 2016).

2.2. Field experiment

Our dataset has been collected during Dynatrez II field experiment in autumn 2016. The campaign was design to shed some light on the short term morphodynamics. Twenty three days of observations, representing a whole neap-spring tidal cycle, have been recorded. The hydrodynamics conditions at the beach have been observed with 17 pressure sensors. 15 sensors have been deployed along a cross shore profile and 2 along a longshore profile. We have used two types of pressure sensor from OSSII, collecting data at a frequency of 10 and 8 hertz. A current meter ADCP (RDI WHS 1200 kHz) and a pressure sensor have been deployed at one kilometer offshore of the beach.

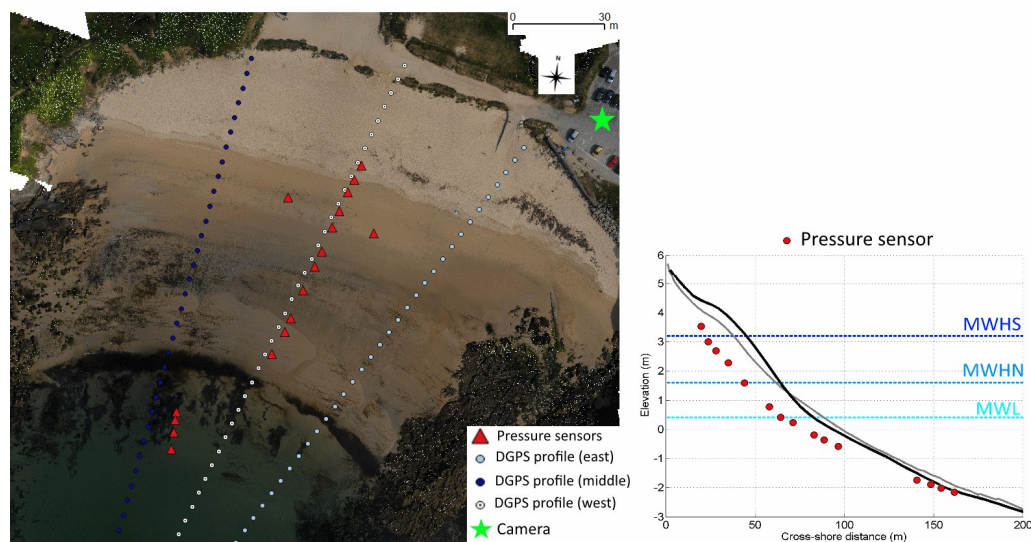


Figure 2. Location of the instruments during the field experiment. Left: disposal of the instruments on the beach: 15 pressures sensors have been deployed along a cross-shore transect (the four devices at the bottom have been shifted from the middle profile due to rock and fossilized peat present on the beach) ; 2 along the longshore direction (red triangles). The camera system is installed upstream the beach at few meters height. Three different DGPS profiles have been measured during the campaign (colored circles). Right: location of the pressure sensors (red circle) along the averaged profile measured during the fieldwork (black line). The 13-years averaged autumn middle profile is shown (gray line). MWL: Mean Water Level; MWHN: Mean Height Water Neap; MHS: Mean Height Water Spring. The Lowest Astronomical Tide is at -3.42 m IGN69.

A continuous monitoring of the beach is done thanks to a camera system installed upstream the site. The camera provides images of the beach in high resolution (1600 x 1200 pixels) at 2 hertz. Besides hydrodynamic observations, daily beach profiles have been acquired via DGPS measurements (Topcon RTK) along three cross shore transects, covering a significant portion of the foreshore (figure 2). These profiles have been measured during each low tide. In the following, a reference to the DGPS profile will concern the middle profile.

2.3. Processing

We describe here the processing we have used to extract the different data used in our study.

2.3.1. Hydrodynamic conditions

The offshore wave conditions have been measured from the data collected by the pressure sensor, located in 20 m depth off the beach. The data collected by the ADCP are not useable since the device has been dredged few days after the deployment. The data have been corrected relative to the atmospheric pressure and shifted to a common reference level (IGN 69) shared by our other observations. We have performed a spectral analysis (Fast Fourier Transform) to the detrended data, separate on 25 minutes segments. The energy spectra have been computed using a cut-off frequency of 0.25 hertz and using a Hanning type window to avoid the noise brings by high frequency fluctuations. From the spectra, we have computed the significant wave height (Eq. 2), the peak period and the wavelength of the offshore waves (noted H_0 , T_p and λ_0 respectively). The wavelength has been computed by inverting the linear relation of dispersion.

$$H_0 = 4 * \sqrt{\sum PSD(f).df} \quad (2)$$

The tide data has been extracted from the pressure sensor measurements using a low pass filter with phase preservation (cut-off frequency equals to 2 hours). From there, the offshore still water (SWL) level has been extracted by averaging the signal every 10 minutes.

The hydrodynamics conditions at the shore are given thanks to a pressure sensor, located at the bottom of the beach (the farthest from the upper beach).

2.3.2. Swash assessment

The cross-shore position of the wave setup can be derived from our video data as often detailed in the literature (Holman et al., 1993 ; Stockdon et al., 2006) from cross-shore 10-minutes time stack extracted on the daily DGPS cross-shore profile projected in the camera coordinate system (Leckler, 2013). From the stacked image converted in grayscale pixels we have determined the position of the water line using differentiation of pixel's intensities.

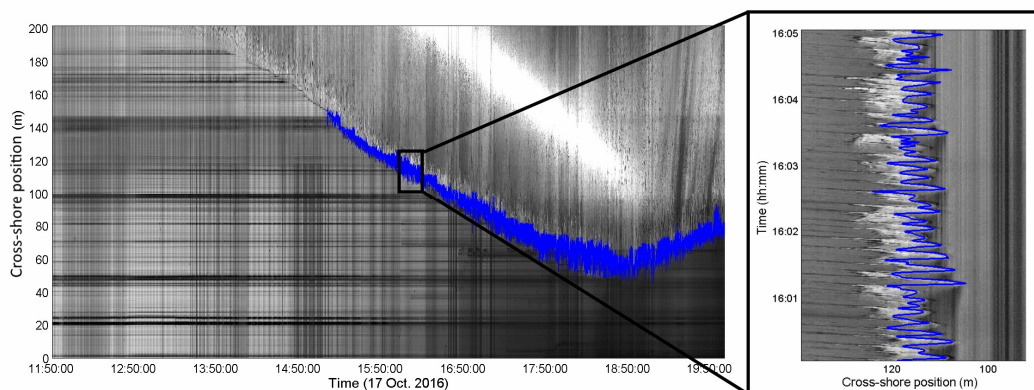


Figure 3. An example of the swash assessment obtained during a whole tidal cycle (17th October 2016). Left: whole capture of the real-time swash excursions during the tide. Right: zoom of the extracted swash time series.

The swash time series has been extracted along 8 whole tides: the 16th, 17th, 18th, 19th, 21st, 22nd, 23rd and

24th of October (an example of these time series is given in figure 3). In order to get the best results we have use different levels of the threshold intensity, determined on a case by case basis. The time series of the water line's position have been then converted to elevation time series, according to the altitude measured with the daily DGPS profile during the low tide. The DGPS profile has been resampled in order to improve the accuracy of the conversion between swash positions and heights (ten times the initial number of points). This leads to increase the resolution of the initial elevation profile. The horizontal pixel's resolution decreases rapidly with the distance between the camera and the observed area. An elevation transect with a resolution of few centimeters [2 to 4 cm] was used while the horizontal resolutions values are between 10 to 90 cm in the foreshore. Since the resolution was too low at the bottom of the beach (i.e. beyond 150 m) none observation has been done in this area.

The offshore still water level is subtracted to the swash elevation time series to get the swash height fluctuation according to the SWL reference. The wave setup is extracted by averaging every 10 minutes of observations. From there we have obtained the runup height by extracting each peak from the swash height time series (figure 4).

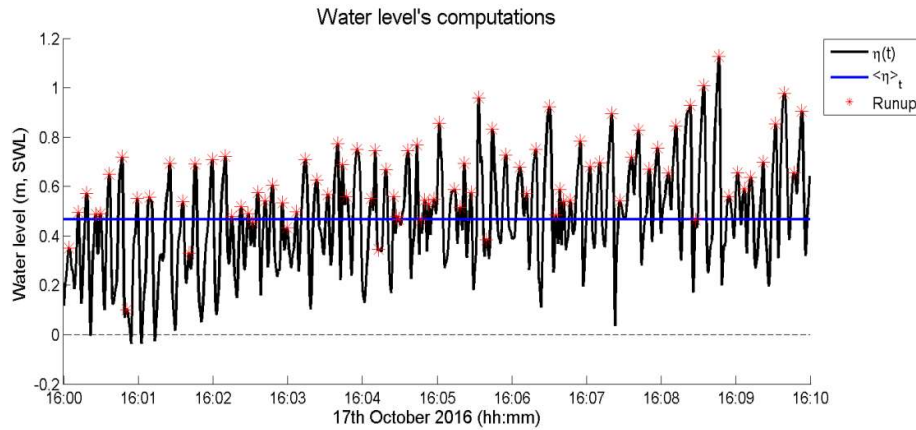


Figure 4. Water level assessment of the swash elevation (noted $\eta(t)$), the wave setup (noted $\langle \eta \rangle_t$), and the runup values (noted R) during 10 minutes of observation.

The runup exceedance ($R_{2\%}$) has been computed by averaging the 2 % biggest runup values. The significant swash height, S , has been extracted (similarly to Eq. 1) according to a spectral analysis (Fast Fourier Transform) over 20 minutes of detrended data: linear trends as well as the mean trends (i.e. here the setup) have been removed. The Fourier Transform has been performed using a cut-off frequency of 0.5 hertz and a Hanning window.

The swash excursion is known to be dependent of the wave frequency (Stockdon et al., 2006 ; Senechal et al., 2011). Therefore, we have separate S in two components corresponding to two frequency bands (Eq. 3: a gravity band ($0.04 < f < 0.5 \text{ Hz}$), noted S_G and an infragravity band containing the low frequency variations ($f < 0.04 \text{ Hz}$) of swash heights, noted S_{IG} .

$$S = \sqrt{S_G^2 + S_{IG}^2} \quad (3)$$

In the whole dataset obtained, more than 11400 swash uprushes have been identified (an average of ~1600 values per tide) and 480 measurements of averaged variables have been extracted (e.g. wave setup, significant height).

2.3.3. Setup and runup empirical models

The wave setup has been investigated in a theoretical way by Miche, 1951 (Miche, 1951). He found that for a monochromatic wave field, the wave setup is restricted to a critical value depending on the beach slope and the wave period. From several field experiments, the wave setup has been investigated regarding to environmental parameters such as the offshore significant waves (Bowen et al., 1968), the Iribarren number (Holman and Sallenger, 1985) or a combination of different parameters (Stockdon et al., 2006). Empirical formulations have been proposed in order to assess the wave setup and runup exceedance. These

expressions are broadly used in coastal engineering field. They provided an assessment of the water level relative to known conditions (i.e. which could be given by numerical models and field properties). Nevertheless the results are contrasted. Early laboratory studies report wave setup values reaching around 20 % of the offshore significant wave height (Bowen et al., 1968; Hedges and Mase, 2004) in accordance with field experiments (Guza and Thornton, 1981; Greenwood and Osbourne, 1990) and theoretical development (Miche, 1951; Longuet-Higgins, [1962, 1963, 1967]). Other field studies show wave setup values greater than the one predicted by the theory (Hansen, 1978; Holman and Sallenger, 1985; Nielsen, 1988; Davis and Nielsen, 1988) or lower (King et al., 1990). These discrepancies are discussed in Raubenheimer et al., 2001, in Dean and Walton (2009) or in Dailloux et al, 2010.

3. Results

3.1. Hydrodynamics parameters conditions

During the field experiment the beach faces low to mild conditions (see figure 5). No energetic events have been recorded.

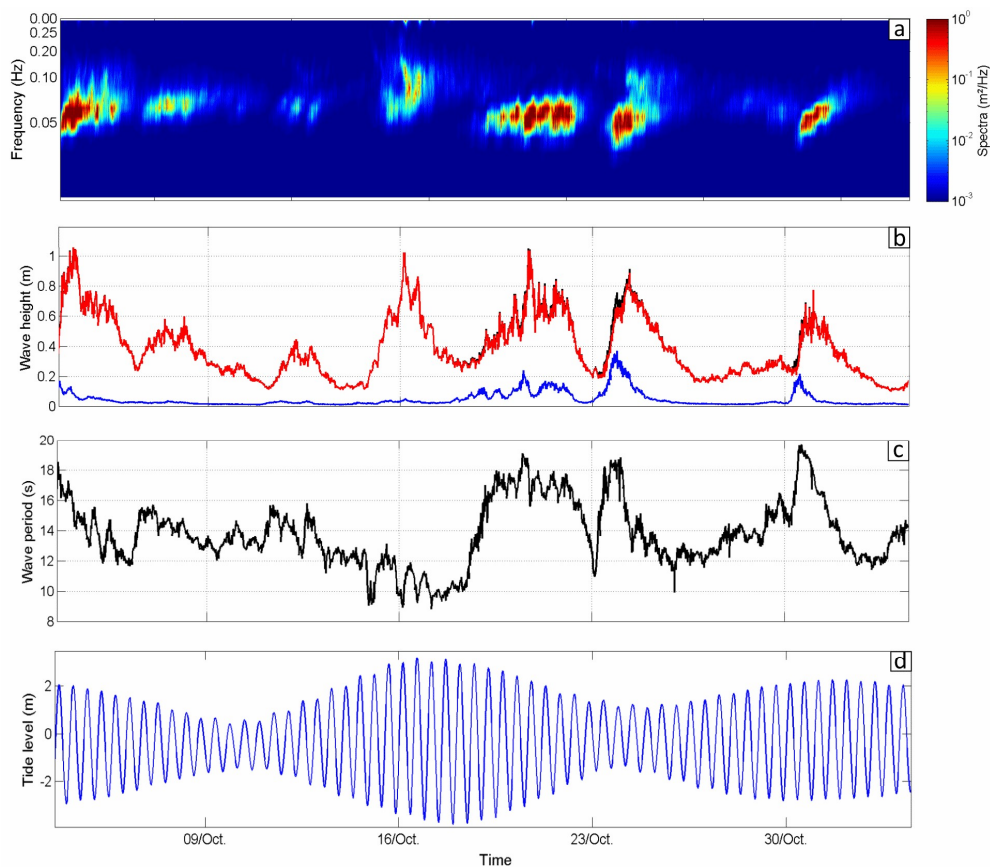


Figure 5. Offshore wave conditions during the field experiment. (a): Spectrum of the offshore pressure (at 20 meters depth). (b) : Offshore significant wave height (black line), significant gravity waves height (red line) and significant infragravity wave height (blue line). (c): Offshore wave period. (d): Tide level (relative to the still water level).

The highest significant wave measured reaches 1.1 m offshore. The same order of magnitude has been recorded at the beach. The offshore period of the wave reaches high value with a peak period equals to 19.6 s (16 s inshore). Four mild regimes have been identified with high peak period (greater than 16 s) and moderate off shore significant waves (H_0 greater than 0.6 m). The tide range reach 7 meters during the

highest tide occurred the 17th of October.

During the experiment, two events of low frequency energy have been recorded. The 23rd and the 31st, we note a remarkable increase of the infragravity waves. The events occurred shortly before increase of wave energy in the gravity band, characterized with quite high peak period (T_p greater than 18 s for the both events). During these two events the ratio between low and high frequency waves (noted $R_{G/IG}$) reaches 50 %, which is greater than the value usually cited in the literature (de Bakker et al. 2014; Inch et al., 2015). Surprisingly these events are not clearly visible on the spectra computed with the pressure sensors located on the beach (the farthest from the upper beach and another located at the MWL). Indeed the highest value of infragravity wave's height is recorded the 24th with a ratio $R_{G/IG}$ around 15 %, which is much lower than the one measured offshore the beach. Moreover no signal of the second event has been captured by the pressure sensors located in the foreshore.

3.2. Beach morphology

The beach profile has slightly changed during the eight days of observation (see figure 6). We have observed an accretion of sand in the upper intertidal zone during the field experiment (between the MHWS limit and the MWL).

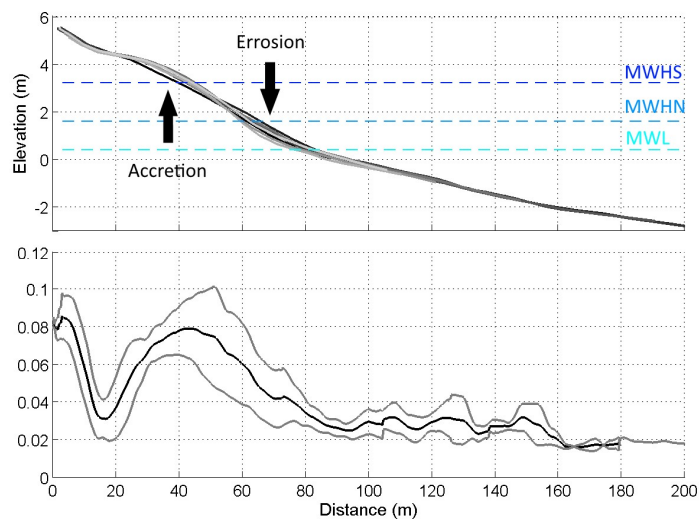


Figure 6. Beach morphology evolutions measured during the campaign. Top: daily DGPS middle profiles. Bottom: beach slope computed along the middle profiles. Black line: mean beach slope during the 8 days of observation. Gray lines highlight the variation of the beach slope during the experiment.

This accretion was accompanied by a beach cups formation, which have evolved and grown all along the campaign. The beach slope changed consequently with an increase in the slope value (+ 25 %) at the MHWN level (~ 60 meters from the top of the beach).

3.3. Setup and runup parametrizations

The highest value of wave setup recorded reaches 0.89 m the 24th of October (5.30 pm), which is in the same order as the significant wave height during the campaign (mean value equals to 0.51 ± 0.18 m), with a maximum value at 0.91 m occurring the same day but in the morning (8.00 am) . In comparison with previous studies discussed above, these ratios of wave setup versus significant wave height are huge.

We have performed several analyses on our in situ dataset to assess the ability of the empirical formulations described above to predict the setup on our study site. Four environmental parameters are used to explore the variabilities of the setup and runup. These parameters form a commonly accepted set of variables. The typical values recorded on the site are presented in table 1.

Table 1. Values of the environmental parameters measured during the 8 days of observations. All the values are

averaged in time, therefore the beach slope values is not clearly representative of the variability observed during the field experiment.

Day	\bar{H}_0 (m)	\bar{T}_p (s)	$\bar{\beta}$	$\bar{\xi}_0$
16 th	0.72 (± 0.08)	11 (± 0.8)	0.057 (± 0.02)	0.77 (± 0.23)
17 th	0.34 (± 0.03)	9.7 (± 0.3)	0.066 (± 0.01)	1.27 (± 0.19)
18 th	0.29 (± 0.02)	11.9 (± 1.3)	0.062 (± 0.02)	1.44 (± 0.50)
19 th	0.47 (± 0.06)	17.0 (± 0.5)	0.062 (± 0.02)	1.39 (± 0.41)
21 st	0.68 (± 0.07)	16.9 (± 0.5)	0.062 (± 0.02)	1.17 (± 0.46)
22 nd	0.36 (± 0.03)	15.6 (± 0.2)	0.071 (± 0.02)	1.70 (± 0.57)
23 rd	0.41 (± 0.14)	17.3 (± 1.0)	0.073 (± 0.03)	2.02 (± 0.89)
24 th	0.73 (± 0.06)	13.8 (± 0.6)	0.063 (± 0.02)	1.00 (± 0.27)

Four examples of the suggested formulatates tested against the in situ data are shown in the figure 7. We have used here the formulation proposed by Stockdon et al., (2006) which are the most common empirical expressions of wave setup and runup exceedance used in civil engineering and in coastal zone management.

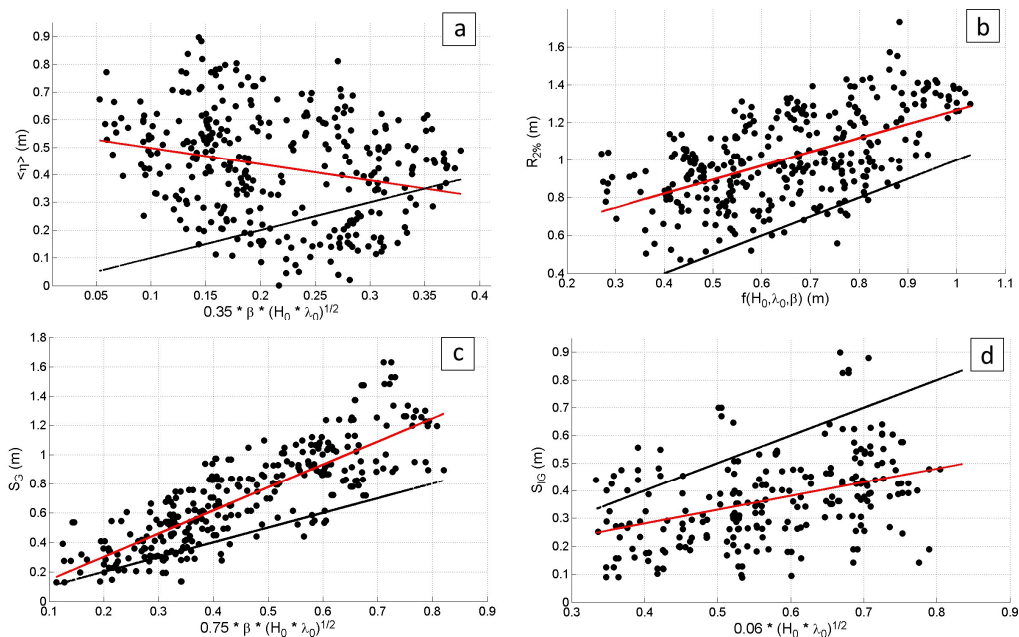


Figure 7. Examples of in situ data tested against the formulations proposed in the literature (black dots). The formulations shown here are suggested by Stockdon et al., (2006). The linear regressions between the in situ data and the models are shown (red lines). Predicted water levels are shown (black lines).

The statistics results of the models are shown in the table 3. For this study, other models have been investigated than those presented in the table 3. We have compared our in situ data to numerous studies: Holman and Sallenger (1985) with a model input for the setup expressed by the Iribarren number times the offshore significant wave height; Yanagishima and Katoh (1990) proposed an expression for the setup similar to the one found by Holman and Sallenger (1985) but with an Iribarren number power 0.4. The in situ wave setup has been assessed with the formulation proposed by Hanslow (1993). The expression suggested by Raubenheimer et al., (2001) for the wave setup linking the significant wave height and the surf zone slope power $-1/3$ has also been investigated. It appears that there are no clear correlations between the in situ measurements of water levels and the models cited in literature. The only clear correlation is obtained by modelling the significant swash height in gravity band by the formulation proposed in Stockdon et al., (2006).

Table 2: Statistics and errors on water level modelling. Different models proposed in the literature are tested. The accordance with our dataset is shown by the correlation coefficient (with a 95 % confidence interval) and by the root mean square error (RMSE) between the model and the in situ data.

Model input	Study	R	RMSE (cm)
$\bar{\eta} = f(H_0)$	Bowen et al. (1968) Hansen (1978) Guza and Thornton (1981)	0.34	17.8
$\bar{\eta} = 0.04 * \sqrt{H_0 * \lambda_0}$	Hanslow and Nielsen (1993)	0.35	17.8
$\bar{\eta} = 0.35 * \beta * \sqrt{H_0 * \lambda_0}$	Stockdon et al. (2006)	- 0.25	18.4
$R_{2\%} = f(\beta, H_0, \lambda_0)$	Stockdon et al. (2006)	0.57	18.9
$S_G = 0.75 * \beta * \sqrt{H_0 * \lambda_0}$	Stockdon et al. (2006)	0.83	18.0
$S_{IG} = 0.06 * \sqrt{H_0 * \lambda_0}$	Stockdon et al. (2006)	0.39	15.5

The correlation coefficient, R, is sufficiently high to indicate that there is a clear link between these two variables. Nevertheless the errors brought by the models are still large (RMSE = 18 cm). Moreover, using the parameters proposed in Stockdon et al., (2006), the setup is not determined correctly at all, with underestimation of 500 %. The runup exceedance is also minimized in large order (100 % in average).

3.2. Morphological and tide response

3.2.1. Morphologic impact

The dissipation effect of the sea floor is stronger on the high frequencies waves (i.e. when the wave steepness is large relative to the beach slope: thus for high Iribarren number value).

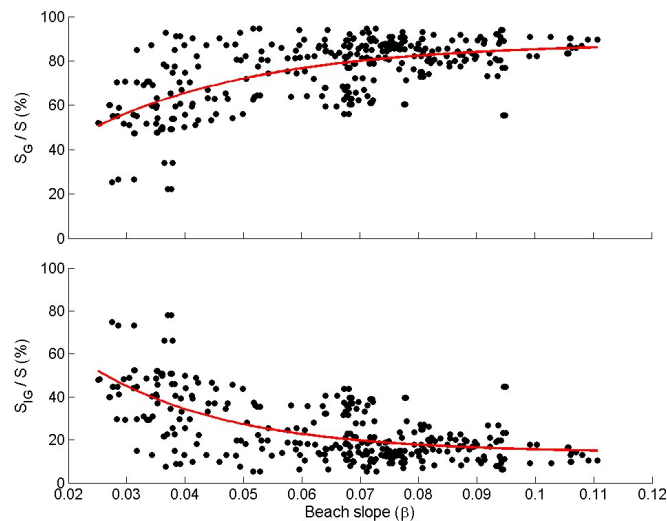


Figure 8. These figures show the evolutions of the swash significant height ratios relative to the beach slope. Top: Evolution of the swash gravity band height ratio. Bottom: Swash infragravity band height ratio (black dots). The red lines are the exponential function fits and are shown to highlight the trends of the data.

For a gently beach slope, the gravity waves is almost fully dissipated which leads usually to a swash zone dynamics driven by the low frequency wave (Russel, 1993; Butt and Russel, 1999). This is visible in our dataset when we look at the swash significant height ratio of S_G and S_{IG} relative to the slope (figure 7). In order to assess if the slope impact was shown on our measurements of water levels, we have drawn the the wave setup and the wave runup) versus the beach slope (figure 7).

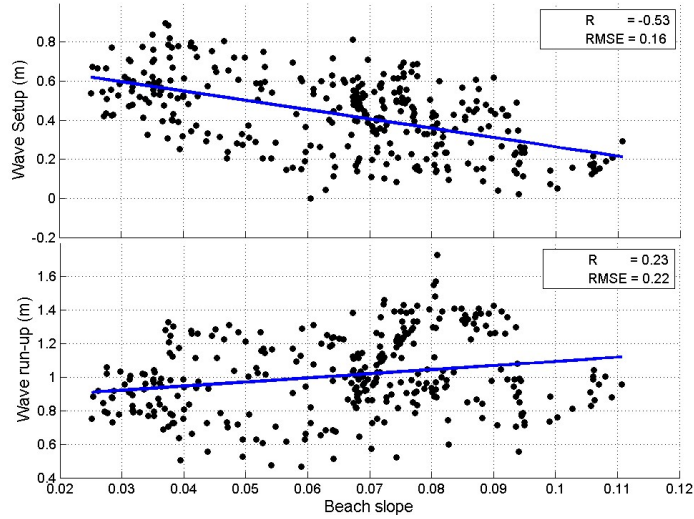


Figure 9. Evolution of the water levels (top panel: wave setup, bottom panel: wave runup) relative to the beach slope (black dots). The linear regressions are drawn (blue lines). The correlation coefficient (R) and root mean square error (RMSE) are indicated.

We have computed the linear regression between these parameters. No clear correlations have been found, in particular for the runup exceedance ($R = 0.23$). Nevertheless the slightly negative trend observed between wave setup and beach slope is opposed to the usual observations reported in the literature (e.g. Bowen et al., 1968; Guza and Thornton, 1981; King et al., 1990). Indeed the sea floor dissipation leads to a global decrease of the water level. Thus in previous experiments the wave setup has been reported to evolve positively with an increase in the beach slope.

3.2.2. Tide modulation

The wave setup evolves differently with the still water level (SWL). Indeed we note that the behavior of the wave setup is de-crescent for a SWL lower than a certain value and crescent on the other side (see figure 10).

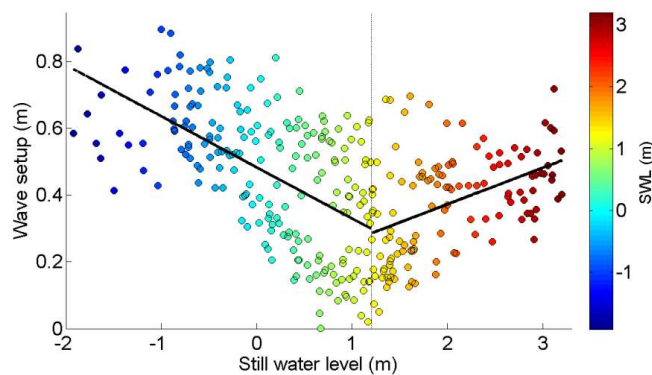


Figure 10. Evolution of the wave setup relative to the still water level (SWL). The trends of the data from either side of a limit (here $SWL = 1.2$ m, gray line) are shown (black lines).

The threshold value is arbitrary and has been chosen by maximizing the correlations between the linear fit and the data from either side (correlations around 0.5). This phenomenon could be driven by the water table dynamics. We have noted that at low tide numerous spots of groundwater exfiltration were present, located at the beach slope discontinuity. This position corresponds more or less to the level used here to

discretize the still water level. The maximum wave setup observed occurred during the lowest tide (tide range equals to 2.6 m) while the lowest value (~ 0 m) occurred during one of the highest tide range (~ 6.6 m).

4. Discussion

The wave setup and the wave runup seem not be correlated to the environmental parameters extracted for the studied site. This nonexistent of links between the water levels and the characteristics of the site (morphologic and or in terms of hydrodynamic forcing) is counter-intuitive and could be questioned. It appears in other studies that the correlations are not always evident (correlation coefficients often lower than 0.6 (Holman and Sallenger, 1985; Stockdon et al., 2006). Moreover the definitions of the environmental parameters as well as the water levels are not totally the same from one study to another. This is particularly true for the beach slope (Raubenheimer et al., 2001).

Nevertheless, the evolutions of the wave setup and wave runup seem to be different from a day to another. Indeed if we discretize the results day per day, the correlation coefficient (R) between the wave setup (or runup exceedance) and the different environmental parameters show a large variability ($R \sim [0 ; 0.7]$). This suggests that local effects can also have large contributions to the wave setup and runup exceedance levels measured on a beach. Nevertheless the behavior of the wave setup regarding to the beach slope is slightly correlated (correlation coefficient up to 0.8), though, negative. This evolution of wave setup is counter-intuitive and contradicts the theory as well as previous observations. This is not the case of the runup exceedance. Quite high correlation coefficients have been found (up to 0.85) and an increase of runup exceedance with the beach slope is found for each day of observation. These remarks are also true for the Iribarren number, which seems to be driven by the beach slope during our experiment.

5. Conclusions

A field experiment has been conducted on a sandy embayed beach. From the in situ dataset, we have analyzed the evolution of the wave setup and wave runup relative to different environmental parameters. The results suggest that the commonly empirical formulations proposed in the literature provide poor assessments of the water levels in this site. Indeed for the site studied here, the predicted wave setup and runup exceedance are underestimated in large proportion (few order of magnitude). Moreover no strong correlations have been found between the whole dataset of these water levels and the environmental parameters extracted for this site ($H_0, \lambda_0, \beta, \xi_0$), although this is nuanced for certain days with large scatter of correlation coefficient values is noted. It suggests that local phenomena could contribute to the wave setup and runup exceedance on this site. Further investigation will be conducted to examine the role of the ground water table on the wave setup.

Acknowledgements

This work was supported by the INSU-SYSTER program of CNRS, the Labex-MER funded by the Agence Nationale de la Recherche under the program « Investissements d'avenir » with the reference ANR-10-LABX-19-01, the lab Géosciences Océan UMR6538 and the Pôle Image zof IUEM. The authors would like to thanks the Géomer and Pôle Image team for their help on the field and the NSO Dynalit/IR ILICO.

References

- Battjes, J. A., 1974. Surf similarity. *Proceedings of the 14th International Conference on Coastal Engineering*, ASCE, (1), 466–480.
- Bergsma, E. W. J., Conley, D. C., Davidson, M. A., & O'Hare, T. J., 2016. Video-based nearshore bathymetry estimation in macro-tidal environments. *Marine Geology*, 374, 31–41.
- Bowen, A. J., Inman, D. L., and Simmons, V. P., 1968. Wave set-down and set-Up. *Journal of Geophysical Research* 73(8).
- Butt, T., Russell, P., 1999. Suspended sediment transport mechanisms in high-energy swash. *Marine Geology*. 161, 361– 375.

- Dailloux, D., Rihouey, D., Dugor, J., Castelle, B., 2010. Analyse critique de l'utilisation des techniques de mesure topographique vidéo comme outil de gestion des plages sableuses. *XIèmes Journées, Les Sables d'Olonne*, January, 449–456.
- Davis, G. A. and P. Nielsen (1988) Field Measurement of Wave Set-up, *ASCE International Conference on Coastal Engineering*, Malaga, Spain, Chapter 38 pp. 539 – 552.
- de Bakker, A., Tissier, M. F. S., and Ruessink, B. G., 2014. Shoreline dissipation of infragravity waves. *Continental Shelf Research*, 72 :73–82.
- Dean, R. G., & Jr, T. L. W., 2008. Wave Setup - A State of Art Review, September, 2008, 1–26.
- Dehouck, A., 2006. Morphodynamique des plages sableuses de la mer d'Iroise (Finistère). PhD thesis, Université de Bretagne Occidentale.
- Floc'h, F., Dantec, N. Le, Lemos, C., Sous, D., Petitjean, L., Arduin, F., Delacourt, C., 2016. Morphological response of a macrotidal embayed beach, Porsmilin, France, *Journal of Coastal Research*, 75, 373–377.
- Greenwood, B. and P. D. Osborne, 1990. Vertical and Horizontal Structure in Cross-shore Flows: An Example of Undertow and Wave Setup on a Barred Beach. *Coastal Engineering*, Vol. 14, pp 543-580. Elsevier Publishing
- Guza, R. T., & Thornton, E. B., 1981. Swash oscillations on a natural beach. *Journal of Geophysical Research: Oceans*, 87(C1), 483–491.
- Hedges, T. S., & Mase, H., 2004. Modified Hunt's Equation Incorporating Wave Setup. *Journal of Waterway, Port, Coastal, and Ocean Engineering*, 130(3), 109–113.
- Hansen, U. A., 1978. Wave Setup and Design Water Level, *Journal of Waterway, Port, Coastal and Ocean Division, American Society of Civil Engineers*, Vol. 104, No. WW2, pp. 227 – 240.
- Hanslow, D.J. and Nielsen, P., 1992. Wave Setup on Beaches and in River Entrances, *23rd International Conference on Coastal Engineering*, Venice, Italy, pp. 240-252.
- Holman, R., Plant, N., & Holland, T., 2013. CBathy: A robust algorithm for estimating nearshore bathymetry. *Journal of Geophysical Research: Oceans*, 118(5), 2595–2609.
- Holman, R. A., & Sallenger, A. H., 1985. Setup and swash on a natural beach. *Journal of Geophysical Research*, 90(C1), 945-953.
- Holman, R., Sallenger, A., Lippmann, T., & Haines, J., 1993. The Application of Video Image Processing to the Study of Nearshore Processes. *Oceanography*, 6(3), 78–85.
- Inch, K., Davidson, M., Masselink, G., and Russell, P., 2015. Field observations of infragravity waves on a on a dissipative, macrotidal beach. *Infragravity waves workshop*, number March.
- Jaud, M. (2011). Techniques d'observation et de mesure haute résolution des transferts sédimentaires dans la frange littorale. PhD thesis, Université de Bretagne Occidentale.
- King, B. A., Carr, A. P., & Hardcastle, P. J., 1990. Observations of wave-induced set-up on a natural beach, 95, 289–297.
- Leckler, F., 2013. Observation et modélisation du déferlement des vagues. Ph.D. Thesis, Université de Bretagne Occidentale.
- Longuet-Higgins, M. S., 1962. Radiation Stress and Mass Transport in Gravity Waves With Application to Surf Beats, *Journal of Fluid Mechanics*, Vol. 13, No. 4, pp. 481 – 504.
- Longuet-Higgins, M. S., Stewart, R.W., 1963. A Note on Wave Set-up, *Journal of Marine Research*, Vol.21, 4-10.
- Longuet-Higgins, M. S., 1967. On the Wave-Induced Difference in Mean Sea Level Between the Two Sides of a Submerged Breakwater, *Journal of Marine Research*, Volume 25, No. 2, pp. 148 – 153
- Masselink G., Castelle B., Scott T., Dodet G., Suanez S., Floc'h F., Jackson D. (2016), Extreme wave activity during 2013/14 winter and morphological impacts along the atlantic coast of Europe, *Geophysical Research Letters*, 43, 2135–2143
- Masselink, G. and Short, A. D., 1993. The Effect of Tide Range on Beach Morphodynamics and Morphology: A Conceptual Beach Model., *Journal of Coastal Research*, 9(3):785-800
- Miche, R., 1951. Le pouvoir réfléchissant des ouvrages maritimes exposés à l'action de la houle. *Annales des Ponts et Chaussées* 121, 285–319.
- Nielsen, P. (1988). Wave Setup: A Field Study, *Journal of Geophysical Research*, Vol. 93(C12), pp. 15, 643-15, 652
- Raubenheimer, B., R. T. Guza, and S. Elgar, 2001 Field Observations of Wave-driven Setdown and Setup, *Journal of Geophysical Research*, 106, C3, 4629-4638.
- Russell, P.E., 1993. Mechanisms for beach erosion during storms. *Continental Shelf Research*. 13, 1243–1266.
- Senechal, N., Coco, G., Bryan, K. R., & Holman, R. A., 2011. Wave runup during extreme storm conditions. *Journal of Geophysical Research*, 116(C7), C07032.
- Stockdon, H. F., Holman, R. A., Howd, P. A., and Sallenger, A. H., 2006. Empirical parameterization of setup, swash, and runup. *Coastal Engineering*, 53(7):573–588.
- Suanez, S., Cancouët, R., Floc'h, F., Blaise, E., Arduin, F., Filipot, J.-F., Delacourt, C., 2015. Observations and Predictions of Wave Runup, Extreme Water Levels, and Medium-Term Dune Erosion during Storm Conditions. *Journal of Marine Science and Engineering*, 3(3), 674–698.
- Yanagishima, S. and K. Katoh, 1990 Field Observation on Wave Setup Near the Shoreline, *Proceedings 22nd International Conference on Coastal Engineering*, Vol.1, Ch. 7, pp. 95-108, ASCE, New York, N.Y.